A COLLOCATED FINITE VOLUME SCHEME WITH AN INTEGRAL FORMULATION FOR FLOWS WITH FLUID SECTION JUMPS

Clément Colas, Martin Ferrand, Jean-Marc Hérard, Erwan Le Coupanec

A COLLOCATED FINITE VOLUME SCHEME WITH AN INTEGRAL FORMULATION FOR FLOWS WITH FLUID SECTION JUMPS

Clément Colas[1,2], **Martin Ferrand**[1,3], **Jean-Marc Hérard**[1,2], **and Erwan Le Coupanec**[1]
[1]EDF R&D, 6 quai Watier 78400 Chatou, France, clement.colas@edf.fr
[2]Aix-Marseille Université, I2M, UMR CNRS 7373, 39 rue Joliot Curie 13453 Marseille, France
[3]CEREA, École des Ponts ParisTech and EDF joint laboratory, 6-8 avenue Blaise Pascal, Cité Descartes Champs-sur-Marne 77455 Marne la Vallée, France

ABSTRACT

We focus here on an integral approach to compute compressible or incompressible fluid flows in physical congested domains with discontinuous fluid sections. This approach is based on a multidimensional integral formulation of the fluid model equations and aims at unifying the porous approach used at component scale and CFD used at local scale. Its discretization uses a semi-implicit collocated finite volume scheme with an incremental pressure-correction algorithm, implemented in the open-source CFD software *Code_Saturne*, version 6.0. Numerical tests are completed by simulating a plane steady-channel flow with a fluid section jump. The results are compared to the analytical solution and the computation obtained with a standard equivalent porous model.

KEYWORDS
Collocated Finite Volume, Euler equations, Pressure-correction scheme, Congested media, Discontinuous fluid sections, Nuclear thermal-hydraulics

1. INTRODUCTION

In this paper we introduce a way to numerically investigate fluid flows in thermal-hydraulic circuit components in nuclear reactors where the computational domain is congested with many axial rod bundles, as the reactor core. The aim is the numerical simulation of channel flow with variable cross section with coarse meshes. An issue is to compute steady state flows in presence of discontinuous cross sections, see Figure 1, sketch of the core entrance. Herein, an integral formulation of the fluid flow governing equations, developed in [1, 2], is used to deal with this flow configuration. This approach demonstrated in [1] its ability to deal with fast transient scenarii and to converge to the CFD solution when refining the mesh. In this framework, the cross section discontinuity is then taken into account in the mesh of the computational domain by a fluid and solid volume in cells and a reduction of fluid surfaces.

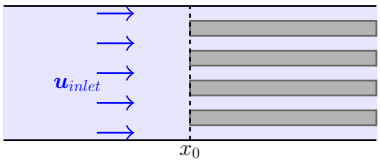

Figure 1. Flow in a congested medium with discontinuous fluid sections at $x = x_0$ with $u_{inlet} \neq 0$.

Nevertheless, the legacy numerical scheme of the integral formulation does not allow to preserve the steady state on either side of the discontinuous interface. This discrepancy is attributed to the fact that the pressure drop at the discontinuous interface is not accounted for in an appropriate way at the discrete level in the momentum balance equation. Indeed, a collocated finite volume scheme in space is used requiring cell value interpolations to approximate the face values. These interpolations do not respect the piecewise smooth profiles of the 1D steady state flow.

The proposed method consists in altering the collocated finite volume scheme in order to take up this discontinuous cross section issue by ensuring the steady state at the discrete level. We initially focus on the Euler equations governing inviscid barotropic compressible fluid flows over a finite time interval $(0,T)$, $T \in \mathbb{R}_+^*$ and in an open connected bounded domain $\Omega \subset \mathbb{R}^d$ ($d = 1, 2$ or 3):

$$\begin{cases} \partial_t \rho + \operatorname{div} \boldsymbol{Q} = 0, \\ \partial_t \boldsymbol{Q} + \mathbf{div}\ (\boldsymbol{u} \otimes \boldsymbol{Q}) + \boldsymbol{\nabla} P(\rho) = 0, \end{cases} \tag{1}$$

where $\boldsymbol{u} : \Omega \times (0,T) \to \mathbb{R}^3$ is the velocity and $P : \Omega \times (0,T) \to \mathbb{R}$, the pressure of the fluid. $\boldsymbol{Q} = \rho \boldsymbol{u}$ denotes the momentum per unit volume with ρ, the density. This system must be supplemented by an equation of state $P(\rho)$, initial conditions and boundary conditions on $\partial\Omega$ for the velocity or the pressure. In this paper, we propose another interpolation of the pressure and the velocity at the internal faces of the mesh, based on the local steady balances over a dual mesh attached to the face of the primal mesh of the computational domain. It allows to enforce the preservation of the discontinuous steady state for flow configurations when fluid section jumps at the interface. A verification test case shows the good behaviour of the new scheme and we compare it to the classical porous approach with a staggered scheme (THYC software, [3]).

2. INTEGRAL FORMULATION

An integral formulation is applied to the Euler equations. Set of equations (1) is integrated over fixed control volumes Ω_i, $i \in \mathbb{N}$, which may potentially contain many disjoint solid obstacles. Before proceeding further, we note that obstacles may be completely or partially included in Ω_i. Part of a control volume boundary may coincide with the surface of an obstacle, see Figure 2 for an example of an obstructed cell. The whole volume occupied by fluid within Ω_i is denoted by Ω_i^ϕ.

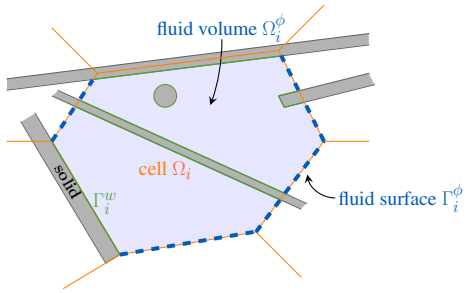

Figure 2. Sketch of a cell including fluid and solid.

The mean value of a quantity $\boldsymbol{\varphi}(\boldsymbol{x},t)$, with $\boldsymbol{x} \in \Omega$ and $t \in \mathbb{R}^+$, within each cell Ω_i of the mesh of Ω, is:

$$\boldsymbol{\varphi}_i(t) = \frac{1}{\left|\Omega_i^\phi\right|} \int_{\Omega_i^\phi} \boldsymbol{\varphi}(\boldsymbol{x},t) \mathrm{d}\boldsymbol{x}. \tag{2}$$

Integrating equations (1) over a bounded time interval $(t^n, t^{n+1}) \subset (0, T)$ and space with respect to the fluid part of the cell Ω_i, for all $i \in \{1, ..., N\}$, gives:

$$\begin{cases} \left|\Omega_i^\phi\right| \left(\rho_i\left(t^{n+1}\right) - \rho_i\left(t^n\right)\right) + \displaystyle\int_{t^n}^{t^{n+1}} \int_{\Gamma_i} \boldsymbol{Q}(\boldsymbol{x},t) \cdot \boldsymbol{n}(\boldsymbol{x}) \mathrm{d}\gamma(\boldsymbol{x}) dt = 0, \\ \left|\Omega_i^\phi\right| \left(\boldsymbol{Q}_i\left(t^{n+1}\right) - \boldsymbol{Q}_i\left(t^n\right)\right) + \displaystyle\int_{t^n}^{t^{n+1}} \int_{\Gamma_i} \left(\boldsymbol{u}\left(\boldsymbol{x},t\right) \boldsymbol{Q}(\boldsymbol{x},t) \cdot \boldsymbol{n}(\boldsymbol{x}) + P\left(\boldsymbol{x},t\right) \boldsymbol{n}(\boldsymbol{x})\right) \mathrm{d}\gamma(\boldsymbol{x}) dt = 0, \end{cases} \tag{3}$$

where $\Gamma_i = \partial\Omega_i^\phi$ denotes the whole boundary of the fluid cell Ω_i^ϕ and $\boldsymbol{n}(\boldsymbol{x})$ its unit outward normal vector.

The slip condition at the wall $\boldsymbol{u} \cdot \boldsymbol{n}|_w = 0$ means that the mass flux is equal to zero through the wall boundary Γ_i^w. Thus, the pressure integral on the wall boundary is the unique contribution. Integral formulation (3) yields by decomposing on the fluid faces $\Gamma_i^\phi = \cup_{j \in N(i)} \Gamma_{ij}^\phi$ and wall Γ_i^w boundaries, for all Ω_i:

$$\begin{cases} \left|\Omega_i^\phi\right| \left(\rho_i\left(t^{n+1}\right) - \rho_i\left(t^n\right)\right) + \displaystyle\int_{t^n}^{t^{n+1}} \sum_{j \in N(i)} \int_{\Gamma_{ij}^\phi} \boldsymbol{Q} \cdot \boldsymbol{n} \mathrm{d}\gamma dt = 0, \\ \left|\Omega_i^\phi\right| \left(\boldsymbol{Q}_i(t^{n+1}) - \boldsymbol{Q}_i(t^n)\right) + \displaystyle\int_{t^n}^{t^{n+1}} \left(\sum_{j \in N(i)} \int_{\Gamma_{ij}^\phi} \left(\boldsymbol{u}(\boldsymbol{Q} \cdot \boldsymbol{n}) + P\boldsymbol{n}\right) \mathrm{d}\gamma \right) dt + \int_{t^n}^{t^{n+1}} \int_{\Gamma_i^w} P\boldsymbol{n} \mathrm{d}\gamma dt = 0. \end{cases} \tag{4}$$

The subscript ij refers to the interface between the neighbouring control volumes Ω_i and Ω_j, with $j \in N(i)$ and $N(i)$ defining the set of neighbouring cells of Ω_i.

3. DISCRETIZATION

The Euler equations are solved with a semi-implicit in time collocated finite volume method, using the same control volumes for both the scalar and the vector unknowns. The algorithm, described below and integrated in the open-source *Code_Saturne* software [4, 5], corresponds to SIMPLEC (Semi-Implicit Method for Pressure Linked Equations-Consistent) algorithm, commonly used to solve the incompressible Navier-Stokes equations, and falls within the class of pressure-correction algorithm, so-called projection methods. A fractional-step method, involving a prediction and a correction of the velocity, is used to solve the momentum conservation and the mass conservation. Numerical fluxes are evaluated by finite volume space schemes [6], considering one approximate mean fluid value $\boldsymbol{\varphi}_i^n$ per cell Ω_i at each discrete time t^n. Many standard first or second order finite volume schemes are available as upwind, centred with or without limiters, SOLU, see [4] for more details. In the sequel, for the sake of simplicity, an upwind scheme is considered.

3.1. Time scheme

We denote $\Delta t = t^{n+1} - t^n$ the time step, between two successive times t^n and t^{n+1} of the time interval $(0, T)$. Starting with ρ^n, $\mathbf{u}^n$ and P^n for all $n \in \mathbb{N}$, momentum balance equation (5) is first solved and provides a predicted velocity $\tilde{\mathbf{u}}$, with a linearisation of the convective flux:

$$\frac{\rho^n \tilde{\mathbf{u}} - \rho^{n-1} \mathbf{u}^n}{\Delta t} + \mathbf{div}\left(\tilde{\mathbf{u}} \otimes \boldsymbol{Q}^n\right) + \boldsymbol{\nabla} P^n = 0. \tag{5}$$

The continuity equation is taken into account during the second step: the mass flux at the faces is corrected by solving semi-discrete equation (6) on the pressure temporal increment:

$$\begin{cases} \dfrac{\rho^{n+1}-\rho^n}{\Delta t} + \text{div}\left(\boldsymbol{Q}^{n+1}\right) = 0, \\ \dfrac{\boldsymbol{Q}^{n+1}-\rho^n\tilde{\mathbf{u}}}{\Delta t} + \boldsymbol{\nabla}\left(P^{n+1}-P^n\right) = 0. \end{cases} \tag{6}$$

Equation (6) is used to update both the mass flux at the faces and the discrete velocity, $\mathbf{u}^{n+1}$.

3.1.1. Prediction step: momentum balance

A predicted velocity field $\tilde{\mathbf{u}}$ is obtained by solving momentum balance equation (5) with a semi-implicit scheme; the velocity is implicit, while the pressure is explicit. The time scheme of the integral formulation of the momentum equation gives for any cell Ω_i:

$$\left|\Omega_i^\phi\right|\left(\rho_i^n\tilde{\mathbf{u}}_i-\rho_i^{n-1}\mathbf{u}_i^n\right)+\Delta t\int_{\Gamma_i^\phi}(\tilde{\boldsymbol{u}}-\boldsymbol{u}^n)\left(\boldsymbol{Q}^n\cdot\boldsymbol{n}\right)\mathrm{d}\gamma=-\Delta t\int_{\Gamma_i^\phi}\boldsymbol{u}^n(\boldsymbol{Q}^n\cdot\boldsymbol{n})\mathrm{d}\gamma-\Delta t\int_{\Gamma_i^\phi\cup\Gamma_i^w}P^n\boldsymbol{n}\mathrm{d}\gamma. \tag{7}$$

In equation (7), we make appear the steady-state momentum balance at the right hand side. This first step provides, for all Ω_i, the unknown $\tilde{\mathbf{u}}_i$, by solving a linear system (using, by default, a block Gauss-Seidel solver). This predicted velocity does not *a priori* fulfill the mass balance.

3.1.2. Correction step: mass balance

The second step, equation (6), corrects the momentum at the faces to impose the mass conservation over the time interval Δt. An implicit scheme of the integral formulation of the mass flux over this time interval, for any cell Ω_i, reads:

$$\left|\Omega_i^\phi\right|\left(\rho_i^{n+1}-\rho_i^n\right)+\int_{\Gamma_i^\phi}\boldsymbol{Q}^{n+1}\cdot\boldsymbol{n}\mathrm{d}\gamma=0. \tag{8}$$

The implicit mass flux $\boldsymbol{Q}^{n+1}\cdot\boldsymbol{n}$ is computed from semi-discrete simplified momentum equation (9) at the fluid interfaces, with $\delta P_i = P_i^{n+1}-P_i^n$ the pressure temporal increment:

$$\boldsymbol{Q}^{n+1}=\rho^n\tilde{\boldsymbol{u}}-\Delta t\boldsymbol{\nabla}\delta P. \tag{9}$$

Besides, the density time variation is linearly approximated with the linear acoustic relation:

$$\rho_i^{n+1}-\rho_i^n=\frac{\delta P_i}{(c_i^2)^n},\ \text{with}\ \ (c_i^2)^n=c^2(\rho_i^n,P_i^n).$$

Thus the integration of Equation (9) gives semi-discrete equation (10):

$$\left|\Omega_i^\phi\right|\frac{\delta P_i}{(c_i^2)^n\Delta t}-\int_{\Gamma_i^\phi}\Delta t\boldsymbol{\nabla}\delta P\cdot\boldsymbol{n}\mathrm{d}\gamma=-\int_{\Gamma_i^\phi}\rho\tilde{\boldsymbol{u}}\cdot\boldsymbol{n}\mathrm{d}\gamma. \tag{10}$$

This second step provides, for all cells Ω_i, the unknown δP_i by solving a linear system. Thus, the pressure is updated such that: $P_i^{n+1}=P_i^n+\delta P_i$ and $\rho_i^{n+1}=\rho_i^n+\frac{\delta P_i}{(c_i^2)^n}$.

Finally, the velocity is corrected with equation (6), which corresponds to the semi-discrete simplified momentum equation (9) written at cells:

$$\mathbf{u}_i^{n+1}=\tilde{\mathbf{u}}_i-\frac{\Delta t}{\left|\Omega_i^\phi\right|\rho_i^n}\int_{\Gamma_i^\phi\cup\Gamma_i^w}\delta P\boldsymbol{n}\mathrm{d}\gamma. \tag{11}$$

3.2. Space scheme

In the following, integral formulation (4) is discretized in space with a cell-centred finite volume scheme. Numerical fluxes are evaluated from the discrete variables to compute the different boundary integrals. We focus on the numerical fluxes on the boundary of a cell intersected by solids.

3.2.1. Prediction step: momentum balance

First the approximation of the convective flux is detailed. The numerical flux is summed on all the fluid interfaces Γ_{ij}^{ϕ} of the cell Ω_i and approximated here by an upwind scheme.

$$\left|\Omega_i^{\phi}\right| \mathbf{div}_i(\tilde{\mathbf{u}} \otimes \boldsymbol{Q}^n) = \int_{\Gamma_i^{\phi}} \tilde{\boldsymbol{u}}(\boldsymbol{Q}^n \cdot \boldsymbol{n}) \mathrm{d}\gamma = \sum_{j \in N(i)} \int_{\Gamma_{ij}^{\phi}} \tilde{\boldsymbol{u}}(\boldsymbol{Q}^n \cdot \boldsymbol{n}) \mathrm{d}\gamma = \sum_{j \in N(i)} \tilde{\boldsymbol{u}}_{ij}^{upw} \left(\boldsymbol{Q}^n \cdot \boldsymbol{n}\right)_{ij} S_{ij}^{\phi}. \tag{12}$$

The mass flux is known from the previous time step, and the implicit convected velocity at the fluid interfaces is $\tilde{\mathbf{u}}_{ij}^{upw} = \lambda_{ij}^n \tilde{\mathbf{u}}_i + (1 - \lambda_{ij}^n)\tilde{\mathbf{u}}_j$, with $\lambda_{ij}^n = 1$ if $\left(\boldsymbol{Q}^n \cdot \boldsymbol{n}\right)_{ij} \geq 0$, $\lambda_{ij}^n = 0$ otherwise.

Second, the approximation of the pressure gradient is detailed. The boundary integral is decomposed on the fluid interfaces and the walls for all cells Ω_i:

$$\left|\Omega_i^{\phi}\right| \boldsymbol{\nabla}_i P^n = \int_{\Gamma_i^w} P^n \boldsymbol{n} \mathrm{d}\gamma + \int_{\Gamma_i^{\phi}} P^n \boldsymbol{n} \mathrm{d}\gamma = \int_{\Gamma_i^w} P_w^n \boldsymbol{n} \mathrm{d}\gamma + \sum_{j \in N(i)} P_{ij}^n S_{ij}^{\phi}. \tag{13}$$

The fluid interface pressure is computed by a linear interpolation of the neighbouring cell pressures:

$$P_{ij}^n = \frac{h_{ij/j} P_i^n + h_{ij/i} P_j^n}{h_{ij/i} + h_{ij/j}} = \alpha_{ij} P_i^n + (1 - \alpha_{ij}) P_j^n. \tag{14}$$

with $\alpha_{ij} = \frac{h_{ij/j}}{h_{ij/i} + h_{ij/j}}$, and $h_{ij/i}$ (respectively $h_{ij/j}$) stands for the distance from the mass centre of the cell Ω_i (respectively Ω_j) to the interface Γ_{ij}^{ϕ}.

For the interior walls of Γ_i^w, a simple alternative for the wall pressure P_w^n approximation is to take the cell value:

$$P_w^n = P_i^n. \tag{15}$$

3.2.2. Correction step: mass balance

Semi-discrete equation (10) is discretized in space by a centred scheme. The explicit mass flux approximation is computed as:

$$\left|\Omega_i^{\phi}\right| \mathrm{div}_i(\rho^n \tilde{\boldsymbol{u}}) = \int_{\Gamma_i^{\phi}} \rho^n \tilde{\boldsymbol{u}} \cdot \boldsymbol{n} \mathrm{d}\gamma = \sum_{j \in N(i)} \int_{\Gamma_{ij}^{\phi}} \rho^n \tilde{\boldsymbol{u}} \cdot \boldsymbol{n} \mathrm{d}\gamma = \sum_{j \in N(i)} (\rho^n \tilde{\boldsymbol{u}})_{ij}^{cent} \cdot \boldsymbol{n}_{ij} S_{ij}^{\phi}, \tag{16}$$

where $\boldsymbol{n}_{ij}$ is the unit outward normal vector at the fluid interface Γ_{ij}^{ϕ} from Ω_i^{ϕ} to Ω_j^{ϕ}. The normal velocity at the fluid interfaces is linearly interpolated between the two neighbouring cell values:

$$(\rho^n \tilde{\boldsymbol{u}})_{ij}^{cent} \cdot \boldsymbol{n}_{ij} = \left(\alpha_{ij} \rho_i^n \tilde{\mathbf{u}}_i + (1 - \alpha_{ij})\, \rho_j^n \tilde{\mathbf{u}}_j\right) \cdot \boldsymbol{n}_{ij}.$$

The pressure gradient increment at the fluid interface is approximated with a "two-point flux approximation" scheme, which is consistent for admissible meshes, see [6, 7]:

$$\boldsymbol{\nabla}\delta P \cdot \boldsymbol{n}_{ij} = \left.\frac{\partial \delta P}{\partial \boldsymbol{n}}\right|_{\Gamma_{ij}^{\phi}} = \frac{\delta P_j - \delta P_i}{h_{ij/i} + h_{ij/j}}.$$

Thus, the scheme yields for the Laplacian operator:

$$-\left|\Omega_i^{\phi}\right| \mathrm{div}_i(\Delta t \boldsymbol{\nabla}\delta P) = -\sum_{j\in N(i)} \int_{\Gamma_{ij}^{\phi}} \Delta t \boldsymbol{\nabla}\delta P \cdot \boldsymbol{n} \mathrm{d}\gamma = -\sum_{j\in N(i)} \frac{\Delta t}{h_{ij/i} + h_{ij/j}} \left(\delta P_j - \delta P_i\right) S_{ij}^{\phi}. \quad (17)$$

Once equation (18) is solved:

$$-\sum_{j\in N(i)} \frac{\Delta t}{h_{ij/i} + h_{ij/j}} \left(\delta P_j - \delta P_i\right) S_{ij}^{\phi} = -\sum_{j\in N(i)} (\rho^n \tilde{\boldsymbol{u}})_{ij}^{cent} \cdot \boldsymbol{n}_{ij} S_{ij}^{\phi}, \quad (18)$$

we deduce the updated mass flux at each fluid interface, satisfying the free-divergence constraint at the discrete level:

$$\sum_{j\in N(i)} \left(\boldsymbol{Q}^{n+1} \cdot \boldsymbol{n}\right)_{ij} S_{ij}^{\phi} = \sum_{j\in N(i)} (\rho^n \tilde{\boldsymbol{u}})_{ij}^{cent} \cdot \boldsymbol{n}_{ij} S_{ij}^{\phi} - \sum_{j\in N(i)} \frac{\Delta t}{h_{ij/i} + h_{ij/j}} \left(\delta P_j - \delta P_i\right) S_{ij}^{\phi} = 0. \quad (19)$$

Rhie & Chow filter is usually added, see [4] for more details.

The velocity update (11) is discretized in space as for the pressure force in equation (7), with a centred scheme:

$$\int_{\Gamma_i^{\phi}\cup\Gamma_i^{w}} \delta P \boldsymbol{n} \mathrm{d}\gamma = \sum_{j\in N(i)} \left(\delta P_{ij}^{cent} - \delta P_i\right) \boldsymbol{n}_{ij} S_{ij}^{\phi}, \quad (20)$$

with: $\delta P_{ij}^{cent} = (1-\alpha_{ij})\delta P_i^n + \alpha_{ij}\delta P_j^n$. The update of the discrete velocity then writes:

$$\mathbf{u}_i^{n+1} = \tilde{\mathbf{u}}_i - \frac{\Delta t}{\left|\Omega_i^{\phi}\right| \rho_i^n} \sum_{j\in N(i)} \left(\delta P_{ij}^{cent} - \delta P_i\right) \boldsymbol{n}_{ij} S_{ij}^{\phi}. \quad (21)$$

As illustrated in §4.3.2 in Figure 5, this scheme does not recover the exact piecewise constant states in 1D configurations when fluid sections jump.

3.3. A new scheme preserving steady state with fluid section jumps

The new scheme consists in modifying the interpolation at the interfaces in order to evaluate numerical fluxes, in the case of a fluid section jump, with the local steady balances in the dual pyramid of each cell.

3.3.1. Dual mesh

A dual mesh, associated to the faces of the primal mesh, is defined with the diamond cells. For each interface ij of the primal cell Ω_i, the two pyramids $\widehat{\Omega}_{i/ij}$ and $\widehat{\Omega}_{j/ij}$ are built, in red in Figure 3, satisfying $\Omega_i = \cup_{j\in N(i)} \widehat{\Omega}_{i/ij}$.

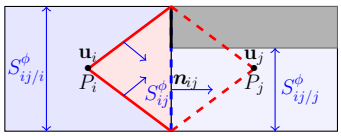

Figure 3. Dual cell and pyramid $\widehat{\Omega}_{i/ij}$.

Thus, the fluid dual-surface vector $\boldsymbol{S}^{\phi}_{ij/i}$ is defined as the fluid surface of the face of the diamond cell in Ω_i such that: $\boldsymbol{S}^{\phi}_{ij/i} = -\int_{(\partial\widehat{\Omega}_{i/ij})^{\phi}\setminus\Gamma^{\phi}_{ij}} \boldsymbol{n}\mathrm{d}\gamma$. The mean value over the dual pyramid $\widehat{\Omega}^{\phi}_{i/ij}$ is also defined as $\boldsymbol{\varphi}_{i/ij} = \dfrac{1}{\left|\widehat{\Omega}^{\phi}_{i/ij}\right|}\displaystyle\int_{\widehat{\Omega}^{\phi}_{i/ij}} \boldsymbol{\varphi}(\boldsymbol{x})\mathrm{d}\boldsymbol{x}$.

3.3.2. Local discrete steady mass balance

The steady mass balance is integrated over the fluid part of the pyramid $\widehat{\Omega}^{\phi}_{i/ij}$ and holds:

$$\left|\widehat{\Omega}^{\phi}_{i/ij}\right| \mathrm{div}_{\,i/ij}(\rho\boldsymbol{u}) = \int_{\widehat{\Omega}^{\phi}_{i/ij}} \mathrm{div}\,(\rho\boldsymbol{u})\,\mathrm{d}\boldsymbol{x} = 0, \tag{22}$$

giving at the discrete level $\rho_i\boldsymbol{u}_{ij/i}\cdot\boldsymbol{n}_{ij}S^{\phi}_{ij} = \rho_i\mathbf{u}_i\cdot\boldsymbol{S}^{\phi}_{ij/i}$, with the approximation $\rho_{ij/i} = \rho_i$. This relation attaches the discrete velocity at cell to the velocity at face in taking into account the ratio of fluid section. We thus define the velocity vector in the dual pyramid as:

$$\boldsymbol{u}_{ij/i} = \left(\mathbf{u}_i\cdot\frac{\boldsymbol{S}^{\phi}_{ij/i}}{S^{\phi}_{ij}}\right)\boldsymbol{n}_{ij} + (\mathbf{Id} - \boldsymbol{n}_{ij}\otimes\boldsymbol{n}_{ij})\,\mathbf{u}_i. \tag{23}$$

3.3.3. Local discrete steady momentum balance

Section jumps imply velocity jumps at interface, and therefore a non-zero convective acceleration term in the steady momentum balance, over the fluid part of the pyramid $\widehat{\Omega}^{\phi}_{i/ij}$. Let us define $\boldsymbol{f}_{i/ij}$, in the pyramid $\widehat{\Omega}^{\phi}_{i/ij}$, the opposite of the discrete convective acceleration due to section jumps:

$$\boldsymbol{f}_{i/ij} = -\frac{\left|\widehat{\Omega}^{\phi}_{i/ij}\right|}{h_{ij/i}S^{\phi}_{ij}}\mathbf{div}_{\,i/ij}\,(\boldsymbol{u}\otimes\boldsymbol{Q})\,. \tag{24}$$

The convective term reads:

$$\begin{aligned}\left|\widehat{\Omega}^{\phi}_{i/ij}\right|\mathbf{div}_{\,i/ij}\,(\boldsymbol{u}\otimes\boldsymbol{Q}) = \int_{\widehat{\Omega}^{\phi}_{i/ij}}\mathbf{div}\,(\boldsymbol{u}\otimes\boldsymbol{Q})\,\mathrm{d}\boldsymbol{x} &= \int_{(\partial\widehat{\Omega}_{i/ij})^{\phi}\setminus\Gamma^{\phi}_{ij}}\boldsymbol{u}(\boldsymbol{Q}\cdot\boldsymbol{n})\mathrm{d}\gamma + \int_{\Gamma^{\phi}_{ij}}\boldsymbol{u}(\boldsymbol{Q}\cdot\boldsymbol{n})\mathrm{d}\gamma\\ &= -\mathbf{u}_i(\boldsymbol{Q}_i\cdot\boldsymbol{S}^{\phi}_{ij/i}) + \mathbf{u}_{ij/i}\,(\boldsymbol{Q}\cdot\boldsymbol{n})_{ij}\,S^{\phi}_{ij}\\ &= \left(\boldsymbol{u}_{ij/i} - \mathbf{u}_i\right)(\boldsymbol{Q}\cdot\boldsymbol{n})_{ij}\,S^{\phi}_{ij}.\end{aligned}$$

Indeed, assuming that the local steady mass balance is verified over the pyramid $\widehat{\Omega}^{\phi}_{i/ij}$, we get:

$$\boldsymbol{Q}_i \cdot \boldsymbol{S}^{\phi}_{ij/i} = (\boldsymbol{Q} \cdot \boldsymbol{n})_{ij}\, S^{\phi}_{ij}.$$

Thus, using equation (23), the projection of equation (24) in the $\boldsymbol{n}_{ij}$-direction gives:

$$\boldsymbol{f}_{i/ij} \cdot \boldsymbol{n}_{ij} = -\frac{(\boldsymbol{Q} \cdot \boldsymbol{n})_{ij}}{h_{ij/i}} \left(\frac{\boldsymbol{S}^{\phi}_{ij/i}}{S^{\phi}_{ij}} - \boldsymbol{n}_{ij} \right) \cdot \mathbf{u}_i. \tag{25}$$

We note that this convective acceleration per unit volume (25), normal to the face, is only non-zero for a fluid section jump. Then, this convective acceleration (25) should be balanced by part of the pressure gradient to satisfy the local discrete steady momentum balance over the cell Ω_i, when the fluid section, between cells Ω_i and Ω_j, is discontinuous.

3.3.4. Pressure interpolation at the interface

The interpolated pressure at face is modified to take into account the fluid section jump at the interface, and thus to recover the steady momentum balance. We assume that the pressure field $P(\boldsymbol{x}, t)$, $\boldsymbol{x} \in \Omega$ and $t > 0$, can be decomposed into two parts, as follows:

$$P(\boldsymbol{x}, t) = P^s(\boldsymbol{x}, t) + P^d(\boldsymbol{x}, t), \tag{26}$$

where P^s is a smooth part, at least $C^1(\Omega)$, and P^d is not necessary $C^1(\Omega)$. Its discrete gradient over the dual pyramid $\widehat{\Omega}^{\phi}_{i/ij}$ is $\boldsymbol{f}_{i/ij}$. At the discrete level, the pressure is also assumed to be split into two parts, over the primal cell Ω_i and Ω_j and at the face centre:

$$\left\{ \begin{array}{l} P_i = P^s_i + P^d_i, \\ P_j = P^s_j + P^d_j, \text{ and } P_{ij} = P^s_{ij} + P^d_{ij}. \end{array} \right. \tag{27}$$

Thus each part of the pressure at the primal faces P^s_{ij} or P^d_{ij} is approximated separately. The pressure P^s_{ij} at each interface is defined by using a linear interpolation between the discrete pressures P_i and P_j:

$$P^s_{ij} = \alpha_{ij} P^S_{out} + (1 - \alpha_{ij}) P^s_j. \tag{28}$$

The pressure $P^d(\boldsymbol{x} \in \widehat{\Omega}^{\phi}_{i/ij})$ is built as a linear function, locally $\mathbb{P}_1$ per pyramid $\widehat{\Omega}^{\phi}_{i/ij}$, with $P^d(\boldsymbol{x}_i) = P^d_i$ and $P^d(\boldsymbol{x}_{\mathtt{f}_{ij}}) = P^d_{ij}$, where $\boldsymbol{x}_{\mathtt{f}_{ij}}$ is the mass centre of the face. We identify the convective acceleration (24) with the pressure gradient per dual pyramid $\widehat{\Omega}^{\phi}_{i/ij}$ and $\widehat{\Omega}^{\phi}_{j/ij}$:

$$\boldsymbol{\nabla}_{i/ij} P^d = \boldsymbol{f}_{i/ij} \text{ and } \boldsymbol{\nabla}_{j/ij} P^d = \boldsymbol{f}_{j/ij}.$$

The pressure P^d is then defined by a first order expansion in the dual pyramids $\widehat{\Omega}_{i/ij}$ and $\widehat{\Omega}_{j/ij}$:

$$\begin{array}{rcl} P^d(\boldsymbol{x}) & = & P^d_i + \boldsymbol{f}_{i/ij} \cdot (\boldsymbol{x} - \boldsymbol{x}_i),\ \forall\, \boldsymbol{x} \in \widehat{\Omega}^{\phi}_{i/ij}, \\ P^d(\boldsymbol{x}) & = & P^d_j + \boldsymbol{f}_{j/ij} \cdot (\boldsymbol{x} - \boldsymbol{x}_j),\ \forall\, \boldsymbol{x} \in \widehat{\Omega}^{\phi}_{j/ij}. \end{array} \tag{29}$$

Then, using decomposition (26) at the interface $P_{ij} = P^s_{ij} + P^d_{ij}$ and equation (28), the pressure at interface reads:

$$P_{ij} = P^s_{ij} + P^d_{ij} = \alpha_{ij} P^s_i + (1 - \alpha_{ij}) P^s_j + P^d_{ij}.$$

Yet, using the decomposition (26) in the cell, $P_i^s = P_i - P_i^d$ and $P_j^s = P_j - P_j^d$, we find:

$$P_{ij} = \alpha_{ij} P_i + (1 - \alpha_{ij}) P_j - \alpha_{ij} P_i^d - (1 - \alpha_{ij}) P_j^d + P_{ij}^d.$$

Finally, equations (29) allow to deduce the expression of the pressure at the interface of mass center $\boldsymbol{x}_{\mathtt{f}_{ij}}$:

$$P_{ij} = \alpha_{ij} P_i + (1 - \alpha_{ij}) P_j + \alpha_{ij} \boldsymbol{f}_{i/ij} \cdot (\boldsymbol{x}_{\mathtt{f}_{ij}} - \boldsymbol{x}_i) + (1 - \alpha_{ij}) \boldsymbol{f}_{j/ij} \cdot (\boldsymbol{x}_{\mathtt{f}_{ij}} - \boldsymbol{x}_j). \tag{30}$$

The first part is the legacy linear interpolation (14) for a continuous pressure and the second is a correction to account for the steady state at an interface with section jump.

3.3.5. Velocity interpolation at the interface

The approximation of the normal velocity at face, projected in the $\boldsymbol{n}_{ij}$-direction (the normal direction to the face ij), is modified in order to comply with the local dual mass balance (23), as follows:

$$\boldsymbol{u}_{ij} \cdot \boldsymbol{n}_{ij} = \frac{\lambda_{ij}^n \mathbf{u}_i \cdot \boldsymbol{S}_{ij/i}^{\phi} + (1 - \lambda_{ij}^n) \mathbf{u}_j \cdot \boldsymbol{S}_{ij/j}^{\phi}}{S_{ij}^{\phi}}, \tag{31}$$

where λ_{ij}^n is deduced from the scheme choice (upwind, centred, ...).

Thus the interpolated velocity at the interface can be rewritten:

$$\boldsymbol{u}_{ij} = \lambda_{ij}^n \boldsymbol{u}_{ij/i} + (1 - \lambda_{ij}^n) \boldsymbol{u}_{ij/j}. \tag{32}$$

Equation (30) (respectively (32)) is used to interpolate the pressure and its increment (respectively the velocity and its increment) in (12), (13), (16) and (20).

4. VERIFICATION TEST CASE: PLANE STEADY-SATE CHANNEL FLOW WITH A DISCONTINUOUS FLUID SECTION

This section is dedicated to the verification of the numerical scheme on steady configurations including a fluid section jump. The aim is to simulate a plane steady-state inviscid fluid flow in a channel with a discontinuous fluid section, see Figure 4. The exact velocity and pressure fields are piecewise constant.

4.1. One-dimensional analytic solution

The problem of the steady plane channel flow with a section jump is considered. The inlet fluid section is denoted by S_{in}, while the outlet fluid section is S_{out}. The inlet mass flow rate $Q_{in} S_{in} \neq 0$ is given, and also the outlet pressure P_{out}. The analytical solution is computed by integrating the steady Euler equations in space with respect to the computational fluid domain Ω^{ϕ}. The density $\rho(x)$, the velocity $u(x)$, the pressure $P(x)$ are assumed to be uniform in the transverse directions to the x-direction. By definition, we have $Q(x) = \rho(x) u(x)$. At the steady state, the mass conservation and momentum balance give:

$$\begin{aligned} Q_{out} S_{out} - Q_{in} S_{in} &= 0, \\ (u_{out} Q_{out} + P_{out})\, S_{out} - (u_{in} Q_{in} + P_{in})\, S_{in} + P_w\, (S_{in} - S_{out}) &= 0. \end{aligned} \tag{33}$$

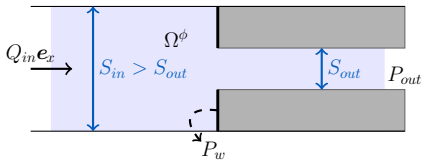

Figure 4. Channel flow with a constriction.

We note $P_w = P_{in} + \Delta P^w$ allowing to write:

$$\left(\frac{Q_{out}^2}{\rho_{out}} - \frac{S_{out}}{S_{in}}\frac{Q_{out}^2}{\rho_{in}}\right) S_{out} + (P_{out} - P_{in})\, S_{out} + \Delta P^w\,(S_{in} - S_{out}) = 0, \tag{34}$$

with $\rho_{out} = \mathcal{P}^{-1}(P_{out},\, h_o)$ and h being the specific enthalpy. We deduce the following equation, for $S_{out} \neq 0$:

$$\frac{S_{out}}{S_{in}}\frac{Q_{out}^2}{\rho_{in}} + P_{in} - \Delta P^w\left(\frac{S_{in}}{S_{out}} - 1\right) = \frac{Q_{out}^2}{\rho_{out}} + P_{out}. \tag{35}$$

The aim is to compute unknown independent variables: for instance, the velocity u_{in}, the pressure P_{in} (the density ρ_{in}, h_{in} for a compressible flow model). Thus, the pressure drop, $P_{in} - P_{out}$, due to the discontinuous section of the channel, will be obtained. This result depends on the parameter ΔP^w, data from the fluid model. For numerical applications, ΔP^w is assumed to be equal to zero, that is $P_w = P_{in}$.

4.1.1. Incompressible fluid flow

For the incompressible Euler equations with $\rho = \rho_{out} = \rho_{in}$ constant, one gets:

$$u_{in} = \frac{Q_{in}}{\rho_{in}} = \frac{S_{out}}{S_{in}}\frac{Q_{out}}{\rho} = \frac{S_{out}}{S_{in}}u_{out}. \tag{36}$$

$$P_{in} = P_{out} + \frac{Q_{out}^2}{\rho}\left(1 - \frac{S_{out}}{S_{in}}\right) + \Delta P^w\left(\frac{S_{in}}{S_{out}} - 1\right). \tag{37}$$

4.1.2. Barotropic compressible fluid flow

For the barotropic compressible Euler equations with the thermodynamic law $P = \mathcal{P}(\rho)$, the equation is implicit. Setting $X = \rho_{in}$, we look for the subsonic zero X of the function f:

$$f(X) = \frac{S_{out}}{S_{in}}\frac{Q_{out}^2}{X} + \mathcal{P}(X) - \Delta P^w\left(\frac{S_{in}}{S_{out}} - 1\right) - \frac{Q_{out}^2}{\rho_{out}} - P_{out}. \tag{38}$$

From the density ρ_{in}, we deduce the pressure $P_{in} = \mathcal{P}(\rho_{in})$ and the velocity $u_{in} = \dfrac{S_{out}}{S_{in}}\dfrac{Q_{out}}{\rho_{in}}$.

Application with an Ideal Gas (IG) equation of state: the reference entropy is $s_0 = 69785$ with $P = s_0\rho^\gamma$ ($\gamma = \frac{7}{5}$).

4.1.3. Compressible fluid flow with energy

The compressible Euler equations with the thermodynamic law $P = \mathcal{P}(\rho, h)$ is considered. The discretization of the energy balance equation is detailed in [1]. At the steady state, in addition to the mass and momentum balance equations, the energy balance equation gives the conservation of the specific total enthalpy: $H_{out} = H_{in}$, where $H_{out} = h(P_{out}, \rho_{out}) + \frac{1}{2}u_{out}^2$ and $H_{in} = h_{in} + \frac{1}{2}u_{in}^2$. We deduce $h_{in} = H_{out} - \frac{1}{2}\frac{S_{out}^2}{S_{in}^2}\frac{Q_{out}^2}{X^2}$. The function f writes:

$$f(X) = \frac{S_{out}}{S_{in}}\frac{Q_{out}^2}{X} + \mathcal{P}\left(X, H_{out} - \frac{1}{2}\frac{S_{out}^2}{S_{in}^2}\frac{Q_{out}^2}{X^2}\right) - \Delta P^w\left(\frac{S_{in}}{S_{out}} - 1\right) - \frac{Q_{out}^2}{\rho_{out}} - P_{out}. \tag{39}$$

We look for the subsonic zero of f allowing to compute ρ_{in} and to deduce $P_{in} = \mathcal{P}\left(\rho_{in}, H_{out} - \frac{1}{2}\frac{S_{out}^2}{S_{in}^2}\frac{Q_{out}^2}{\rho_{in}^2}\right)$ and $u_{in} = \frac{S_{out}}{S_{in}}\frac{Q_{out}}{\rho_{in}}$.

Application with an ideal gas equation of state, $h = \frac{\gamma}{\gamma-1}\frac{P}{\rho}$: one have $\mathcal{P}(X) = \frac{\gamma-1}{\gamma}X\left(H_{out} - \frac{1}{2}\frac{S_{out}^2}{S_{in}^2}\frac{Q_{out}^2}{X^2}\right)$. For $\gamma = \frac{7}{5}$, we compute $\rho_{in} = 47.4599\ kg/m^3$ and deduce $h_{in} = 1143810.0776143975\ J/kg$.

variable	incomp.	IG baro.	IG ener.
$\rho_{in}\ (kg/m^3)$	47.5	47.4582	47.4599
$P_{in}\ (Pa)$	15509500	15509501.88649098	15510031.972163301
$u_{in}\ (m/s)$	10	10.008807750820722	10.008449238198985
Out state	$\frac{S_{in}}{S_{out}} = 2$	$P_{out} = 155$ *bar* and $Q_{in}S_{in} = Q_{out}S_{out} = 475$ *kg/s* $\rho_{out} = 47.437\ kg/m^3$	

4.2. Standard porous approach: THYC component code

Numerical computations are compared to the reference porous code THYC for thermal-hydraulic simulation at the component scale [3]. Set of equations (40), based on the barotropic compressible Euler equations, is the porous model involving a steady porosity ε:

$$\begin{cases} \partial_t(\varepsilon\rho) + \text{div}\,(\rho\varepsilon\boldsymbol{u}) = 0, \\ \partial_t(\varepsilon\rho\boldsymbol{u}) + \textbf{div}\,(\boldsymbol{u}\otimes\varepsilon\rho\boldsymbol{u}) + \varepsilon\boldsymbol{\nabla}P = 0. \end{cases} \tag{40}$$

The discretization uses a staggered space scheme on a Cartesian grid and an incremental pressure-correction time algorithm. In this model, the pressure drop, at the channel fluid section jump, is dealt with the non-conservative term $\varepsilon\boldsymbol{\nabla}P$. The approximation of the porosity at the discontinuous interface, $x = x_0$, controls the pressure drop value: $\varepsilon = \frac{1}{2}(\varepsilon_{in} + \varepsilon_{out})$ is used here. The other approximation $\varepsilon = \min(\varepsilon_{in}, \varepsilon_{out})$ is actually relevant and allows to recover the analytic solution.

4.3. Numerical results

4.3.1. Case description

The one-dimensional computational domain $\Omega = (0, 40\ m)$ is meshed with a uniform Cartesian grid with N cells, $N = 10, 80$ or 1280. The jump section is located at $x = 0\ m$. The section ratio is $\frac{S_{in}}{S_{out}}$. The initial

conditions are: $\forall\ x \in \Omega$, $u(x, t = 0) = 0\ m.s^{-1}$ and $P(x, t = 0) = P_0 = P_{out}$. The computations are performed with a constant time step complying with $CFL_u = \frac{u_{in}\Delta t}{\Delta x} \leq 1$. The boundary conditions are a Dirichlet condition on the mass flow on $\partial\Omega^{in}$, a Dirichlet condition on the pressure on $\partial\Omega^{out}$, and a slip condition, implying $\boldsymbol{u} = u\,\boldsymbol{e}_x$, on $\partial\Omega^{wall}$.

4.3.2. Results

For steady-state incompressible flows, the analytical piecewise constant fields are recovered with the solver precision (10^{-12}) for the velocity and the pressure (see Figure 5) for different mesh refinements. The discrete L^2 error* is 10^{-12} and the L^2 time residuals of the velocity and the pressure are zero (machine precision is obtained). In the case of $\frac{S_{in}}{S_{out}} = 2$, for instance, with $N = 10$, the time convergence is reached after 63 iterations. The discrete pressure errors, in function of the cell centres x_i, are given in Table I. For the other section ratios, the velocity and pressure profiles are given in Figures 6 and 7 and the discrete pressure error in Table I for the inlet condition $u_{in} = 1\ m.s^{-1}$.

Profiles in Figure 8, for $\frac{S_{in}}{S_{out}} = 2$, compare the results obtained with different models (incompressible or compressible flows) and software (*Code_Saturne* or THYC) for $Q_{in}S_{in} = 475\ kg.s^{-1}$ and $P_{out} = 155\ bar$.

Table I. Steady-state discrete pressure errors (*Code_Saturne* incompressible).

Config.	$x_i\ (m)$	2	6	10	14	18	22	26	30	34	38
$\frac{S_{in}}{S_{out}} = 2$	$\lvert P_i - P_{exact}\rvert\ (Pa)$	1.3e-11	2.8e-11	1.6e-11	1.2e-11	1.4e-11	6.7e-12	2.0e-12	2.3e-12	2.3e-12	8.9e-13
$\frac{S_{in}}{S_{out}} = 10$	$\lvert P_i - P_{exact}\rvert\ (Pa)$	4.7e-10	3.6e-10	1.9e-10	1.0e-11	9.8e-11	5.3e-11	2.8e-10	3.4e-10	2.9e-10	1.2e-10
$\frac{S_{in}}{S_{out}} = 100$	$\lvert P_i - P_{exact}\rvert\ (Pa)$	1.7e-9	1.1e-9	1.6e-10	6.6e-10	1.1e-9	3.9e-9	2.1e-9	2.3e-9	1.8e-9	7.0e-10

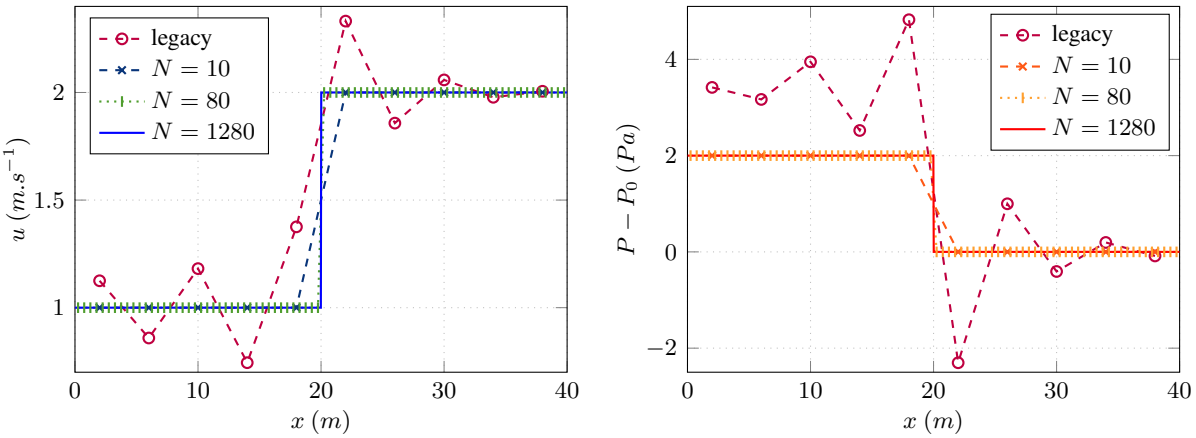

(a) Velocity (b) Pressure

Figure 5. Steady approximate solutions for $\frac{S_{in}}{S_{out}} = 2$ (*Code_Saturne* incompressible).

*The discrete relative L^2 error is defined as: $e_{L^2(\Omega)}(\varphi) = \sqrt{\frac{\sum_{i=1}^{N}\left|\varphi_i^{exact} - \varphi_i^{computed}\right|^2\left|\Omega_i^{\phi}\right|}{\sum_{i=1}^{N}\left|\varphi_i^{exact}\right|^2\left|\Omega_i^{\phi}\right|}}$.

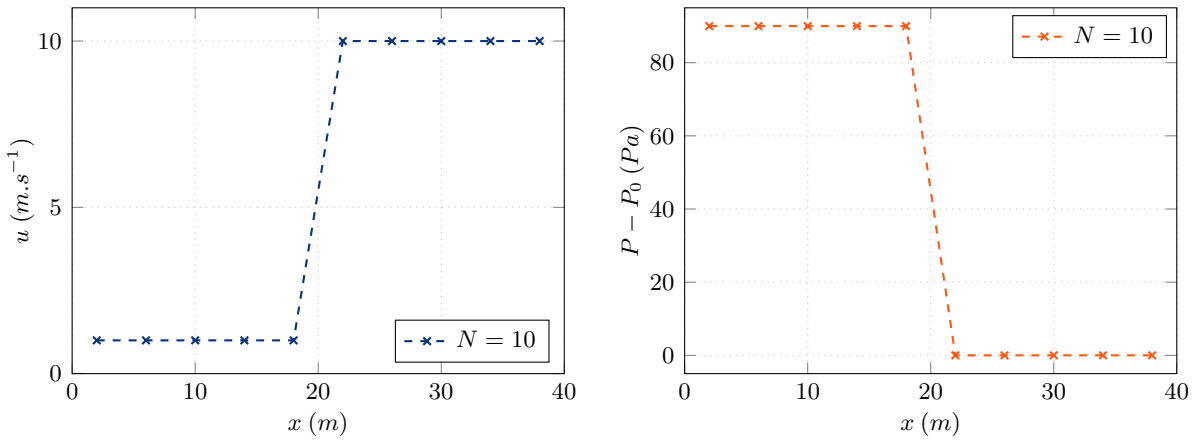

(a) Velocity (b) Pressure

Figure 6. Steady approximate solutions for $\frac{S_{in}}{S_{out}} = 10$ (*Code_Saturne* incompressible).

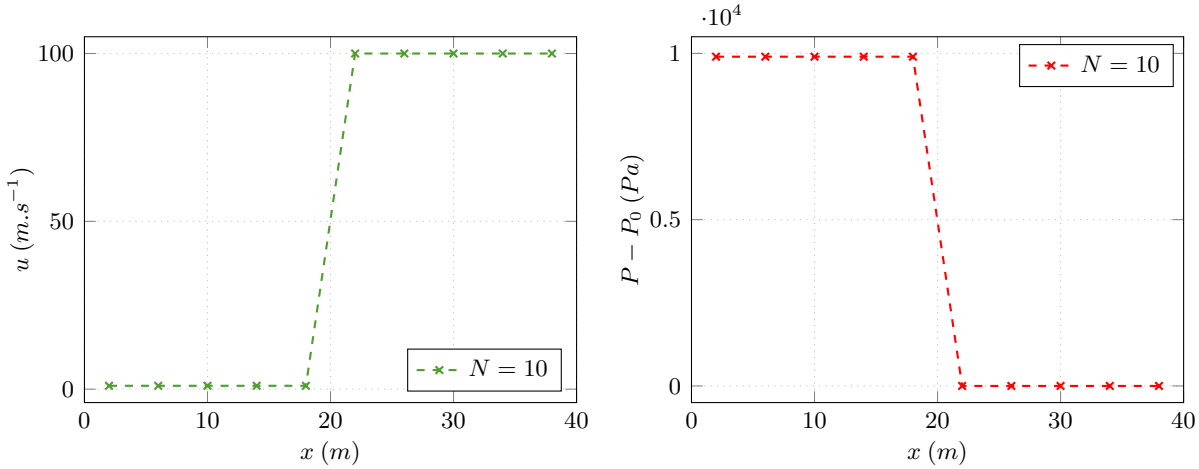

(a) Velocity (b) Pressure

Figure 7. Steady approximate solutions for $\frac{S_{in}}{S_{out}} = 100$ (*Code_Saturne* incompressible).

5. Conclusion

A multi-dimensional integral formulation has been proposed to approximate solutions of the Euler equations in a medium with fluid section jumps on coarse meshes. The discontinuous geometry of the fluid section does not need to be explicitly meshed by using a wall boundary condition. The integral formulation is discretized by a semi-implicit collocated finite volume scheme using an incremental pressure projection method. The proposed space scheme corrects the interpolation at the interface of both the velocity and the pressure. This technique is based on the discrete local steady balance equations over a dual sub-mesh, similarly to a staggered scheme. Numerical verification tests show the ability of the scheme to recover the analytic steady-state flow solution. Indeed, the analytic piecewise constant solution is recovered on a collocated mesh with the correct pressure drop and acceleration at the discontinuous interface. Even if only illustrated on a one-dimensional case in this paper, this scheme is applicable to multi-dimensional computations and its impact will decrease when refining the mesh in all directions. Additional *ad hoc* head

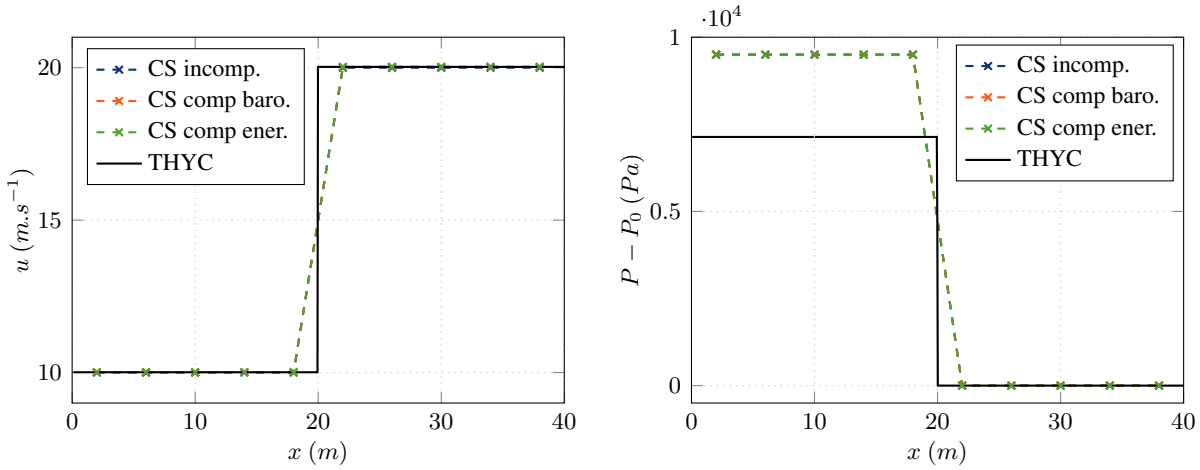

(a) Velocity

(b) Pressure

Figure 8. Comparison of steady approximate solutions between THYC and *Code_Saturne* for $\frac{S_{in}}{S_{out}} = 2$.

loss correlations could be added to the present developments.

ACKNOWLEDGMENTS

The first author receives a financial support by ANRT through an EDF-CIFRE contract 2016/0728. We thank O. Touazi (EDF R&D) for having provided the THYC software results. We also would like to thank T. Gallouët, R. Herbin and J.-C. Latché (Aix-Marseille Université) for fruitful discussions and advice they gave about this work.

REFERENCES

1. C. Colas, M. Ferrand, J.-M. Hérard, J.-C. Latché, and E. Le Coupanec, "An Implicit Integral Formulation to Model Inviscid Fluid Flows in Obstructed Media," *Computers & Fluids*, **188**, pp. 136–163 (2019).
2. J.-M. Hérard and X. Martin, "An integral approach to compute compressible fluid flows in domains containing obstacles.," *International Journal on Finite Volumes*, **12** (1), pp. 1–39 (2015).
3. S. Aubry, C. Caremoli, J. Olive, and P. Rascle, "The THYC three-dimensional thermal-hydraulic code for rod bundles: recent developments and validation tests," *Nuclear technology*, **112** (3), pp. 331–345 (1995).
4. EDF R&D, *Code_Saturne* 6.0 Theory Manual, *available on https://code-saturne.org/* (2019).
5. F. Archambeau, J.-M. Hérard, and J. Laviéville, "Comparative study of pressure-correction and Godunov-type schemes on unsteady compressible cases," *Computers & Fluids*, **38**, pp. 1495–1509 (2009).
6. R. Eymard, T. Gallouët, and R. Herbin, "Finite Volume Methods," *Handbook for Numerical Analysis, P.G. Ciarlet, J.L. Lions eds, North Holland*, **7**, pp. 713–1020 (2006).
7. R. Eymard, T. Gallouët, C. Guichard, R. Herbin, and R. Masson, "TP or not TP, that is the question," *Computational Geosciences*, **18**, pp. 285–296 (2014).